

Efficient detection of Al^{3+} and $\text{B}_4\text{O}_7^{2-}$ over trigonal prism $\text{In}(\text{III})$ complex

Rui Wang,^a Nan Jiang,^a Rong Luo,^a Hai-Jun Yu,^a Yi Yin,^a Shuang-Yu Bi,^b Dong-Mei Zhang,^a and Feng Shao^{*a}

^aKey Laboratory of Marine Chemistry Theory and Technology, Ministry of Education, College of Chemistry and Chemical Engineering, Ocean University of China, Qingdao 266100, China

^bState Key Laboratory of Microbial Technology, Shandong University, Qingdao 266237, China

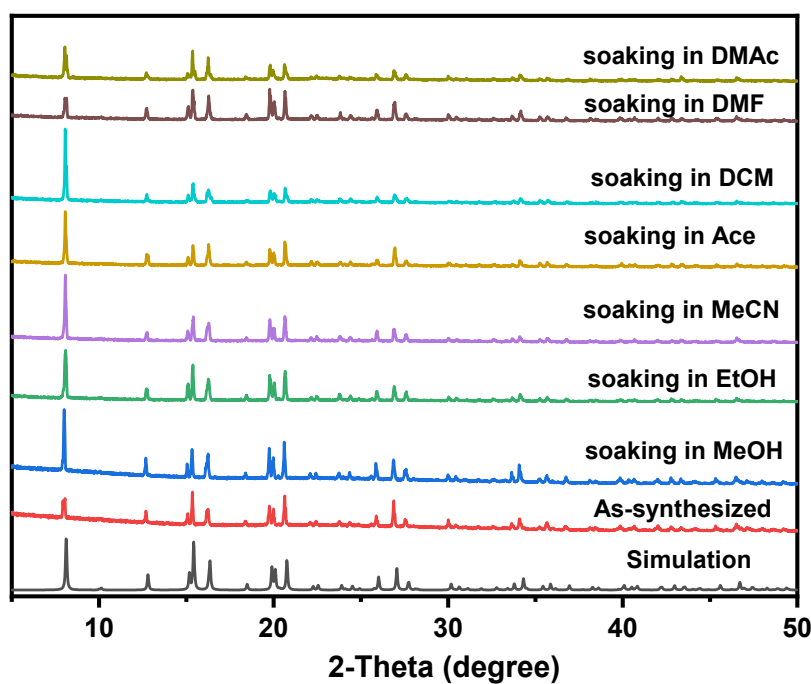


Fig. S1 The Powder X-ray diffraction patterns of **1** immersing in common solvents: methanol (MeOH), *N,N*-dimethylformamide (DMF), *N,N*-dimethylacetamide (DMAc), ethanol (EtOH), acetonitrile (MeCN), dichloromethane (DCM) and acetone (Ace) for 24 h.

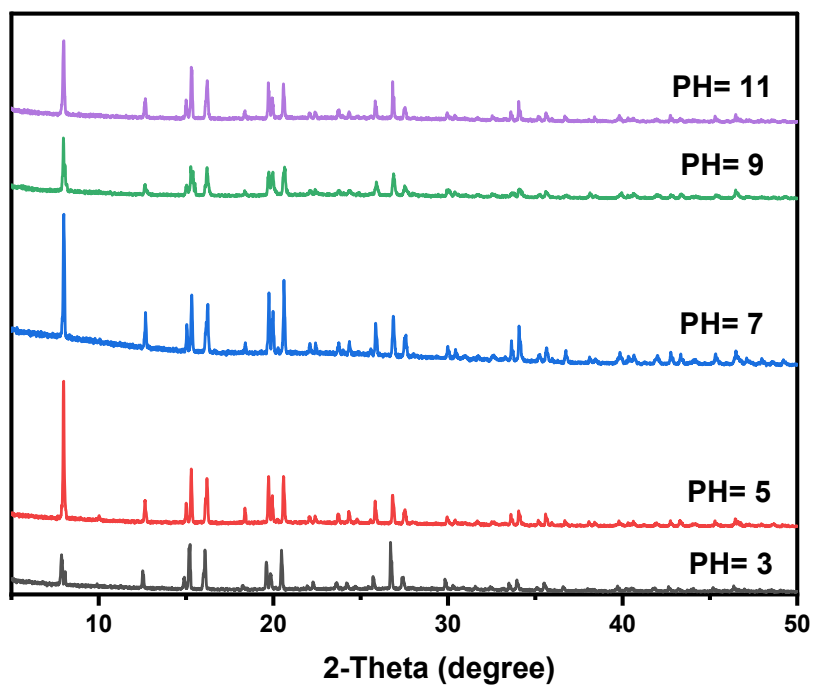


Fig. S2 The Powder X-ray diffraction patterns of **1** immersing in MeOH in different PH values.

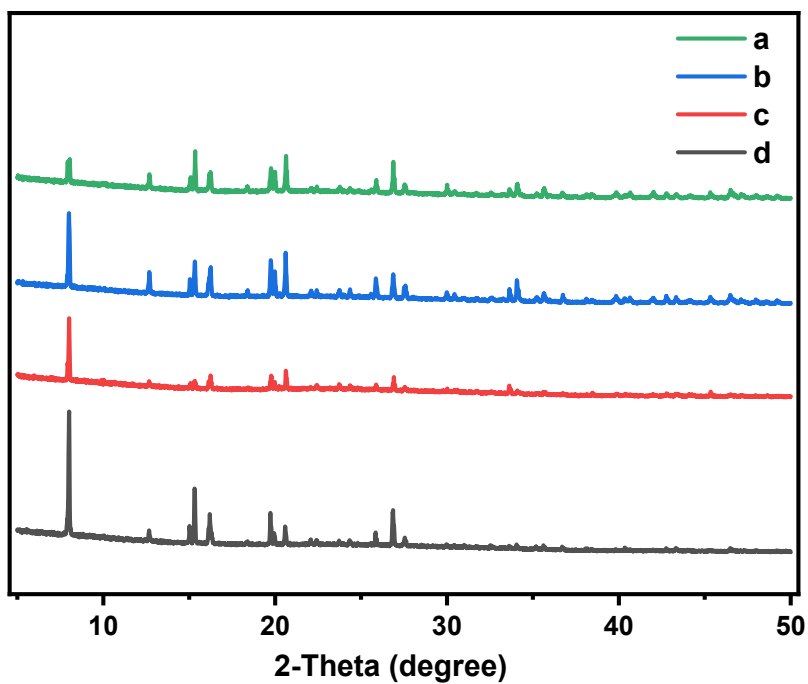


Fig. S3 The PXRD patterns of (a) as-synthesized. (b) **1** after soaked in MeOH for 48 h. (c) **1** after ultrasonic sound in MeOH containing Al^{3+} (10^{-3} M) for 25 min. (d) **1** after ultrasonic sound in MeOH containing $\text{B}_4\text{O}_7^{2-}$ (10^{-3} M) for 25 min.

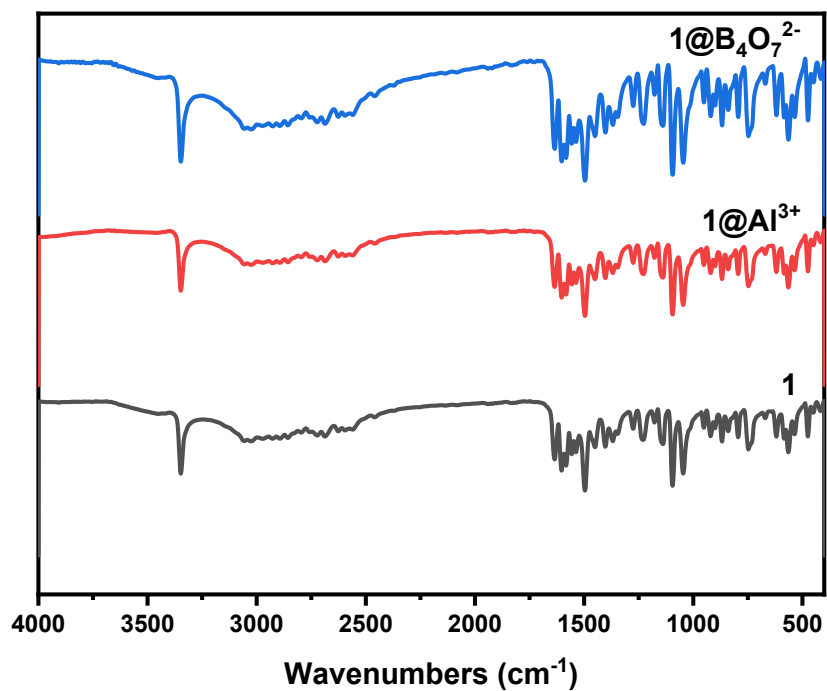


Fig. S4 The FT-IR spectra of **1** before and after being ultrasonic in MeOH containing Al³⁺ and B₄O₇²⁻.

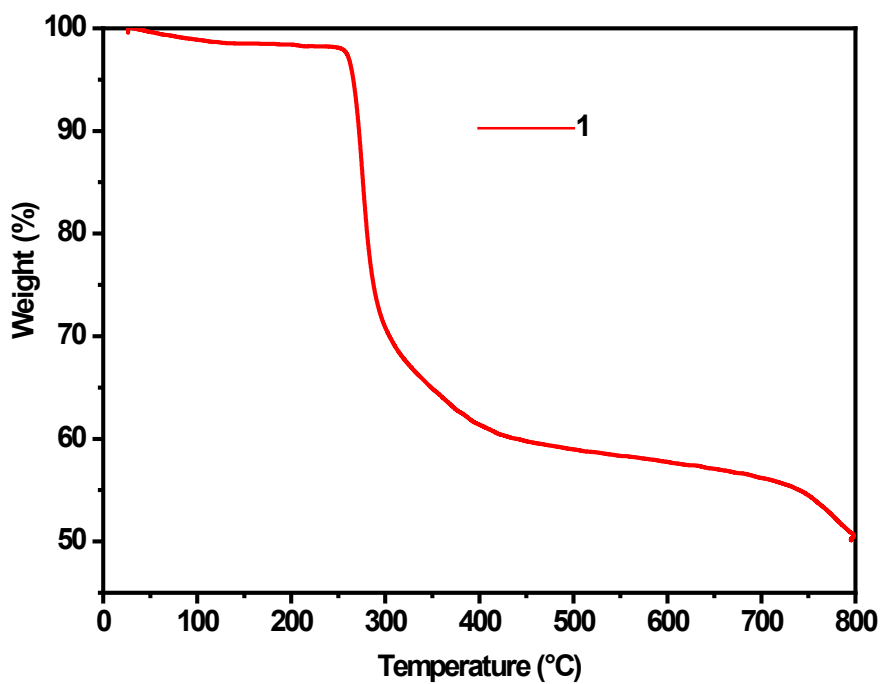


Fig. S5 TGA plot of **1** under N₂ condition.

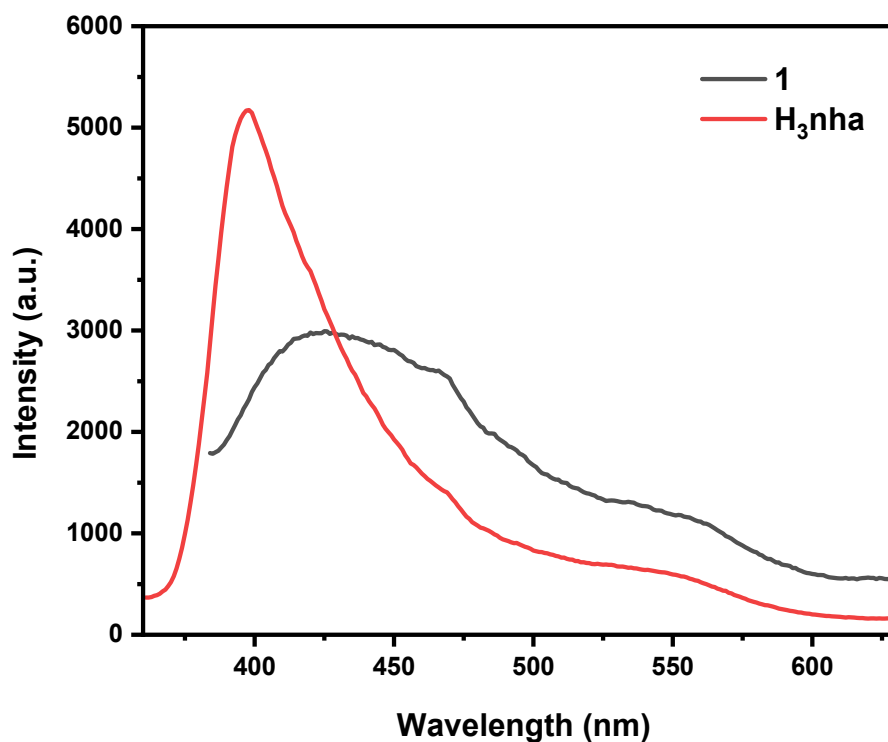


Fig. S6 Solid state luminescence spectra of H₃nha (λ_{ex} =325 nm,) and **1** (λ_{ex} =330 nm)

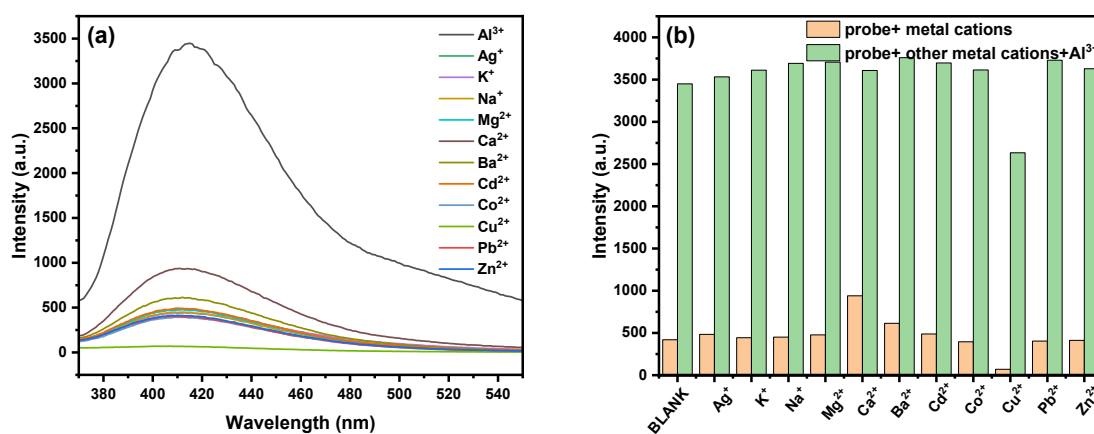


Fig. S7 (a) Luminescence spectra of H₃nha (10^{-4} M) in MeOH upon the addition of different metal ions; (b) Luminescence intensities at 325 nm of H₃nha (10^{-4} M) in MeOH in the presence of only Al³⁺ (10^{-3} M) and Al³⁺ with the other metal ions (10^{-3} M).

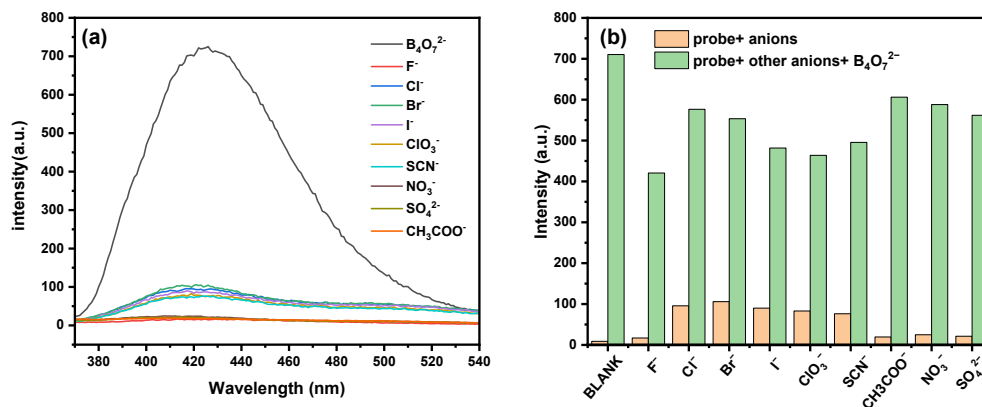


Fig. S8 (a) Luminescence spectra of H_3nha (10^{-4} M) in solution (MeOH:H₂O, v/v =9:1) upon the addition of different non-metal anions; (b) Luminescence intensities at 325 nm of H_3nha (10^{-4} M) in solution (MeOH:H₂O, v/v = 9:1) in the presence of only $B_4O_7^{2-}$ (10^{-3} M) and $B_4O_7^{2-}$ with the other anions (10^{-3} M).

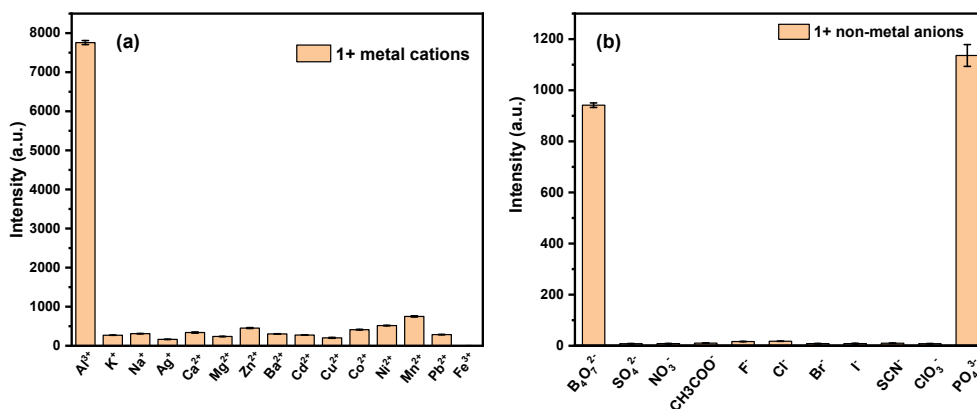


Fig. S9 Luminescence spectra of **1** in MeOH upon the addition of (a) different metal ions and (b) different non-metal anions;

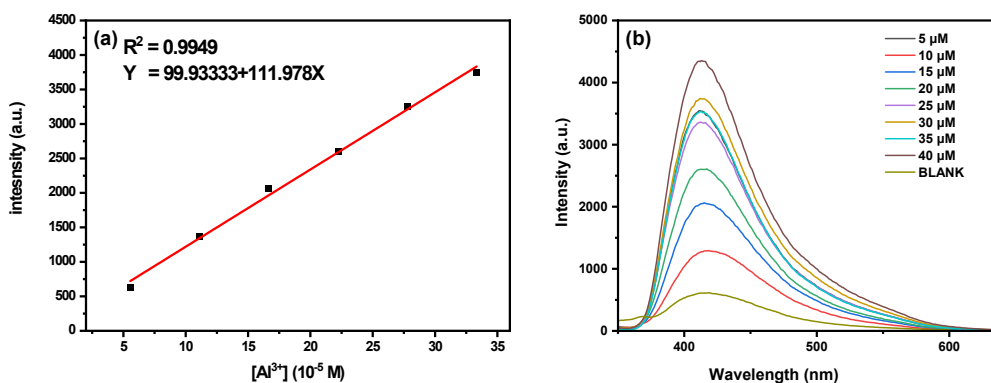


Fig. S10 (a) Linear relationship of the luminescence intensity at 330 nm of **1** with the concentration of Al^{3+} . (b) The luminescence spectra of **1** in MeOH with different concentration of Al^{3+} .

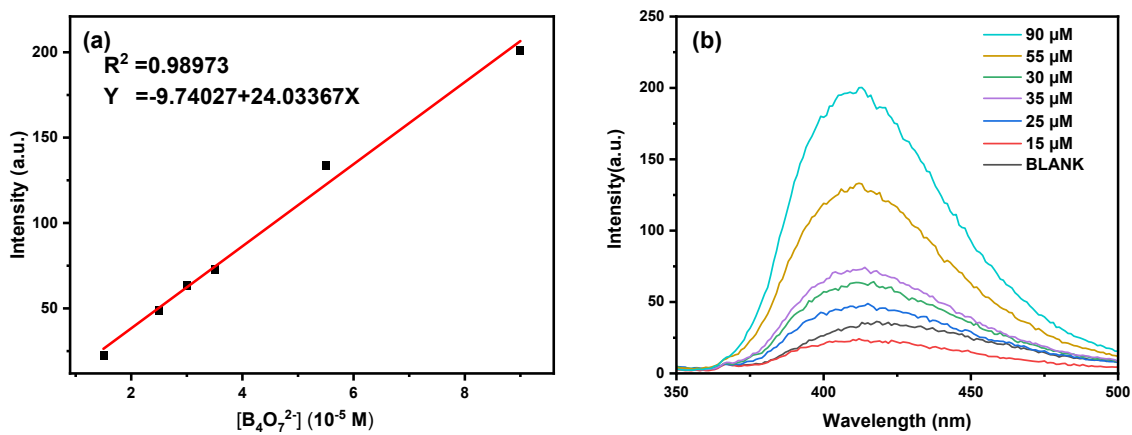


Fig.S11 (a) The luminescence spectra of **1** in solution (MeOH:H₂O, v/v =9:1) with different concentration of B₄O₇²⁻ (b) Linear relationship of the luminescence intensity at 330 nm of **1** with the concentration of B₄O₇²⁻.

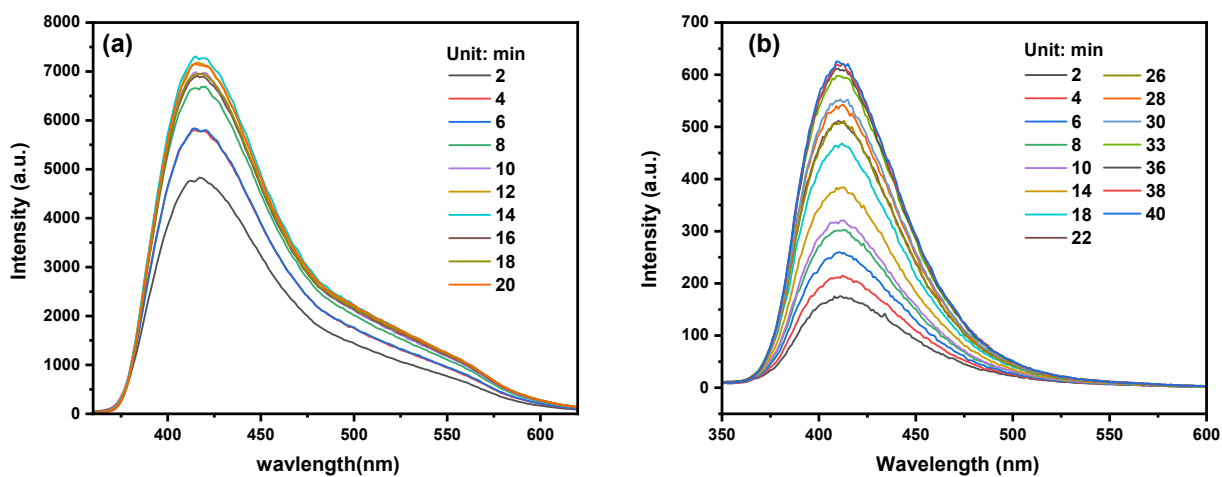


Fig.S12 The luminescence intensity of (a) **1**@Al³⁺ and (b) **1**@B₄O₇²⁻ with the increase of time.

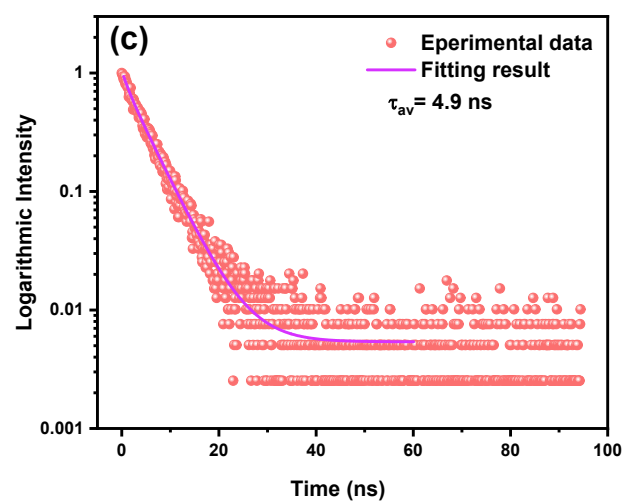
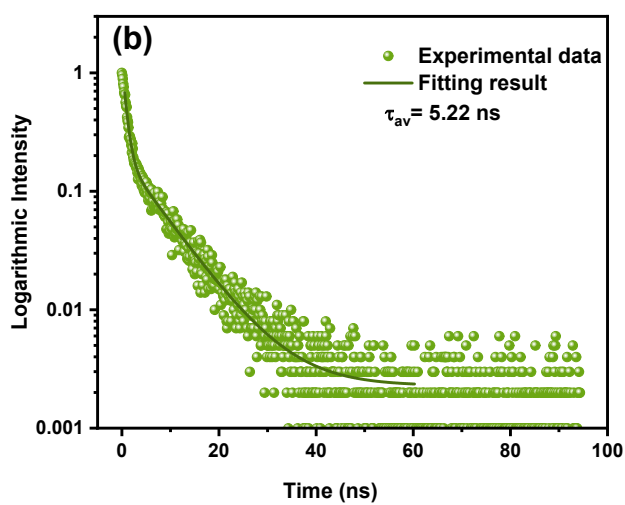
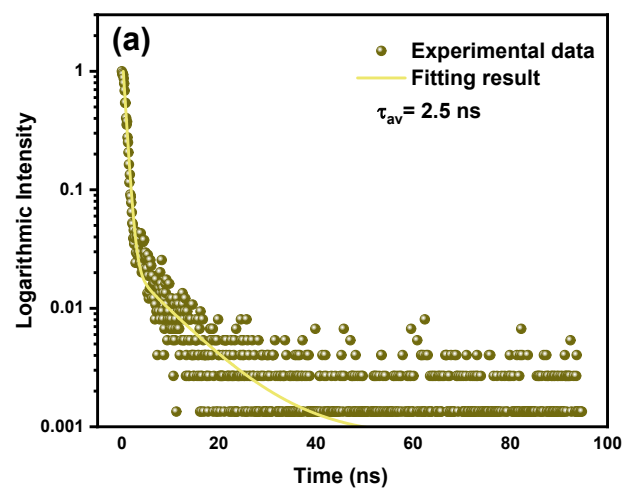


Fig. S13 The time resolved luminescence decay corresponding fitted lines of **1** (a) in MeOH, (b) **1**@Al³⁺, (c) **1**@B₄O₇²⁻.

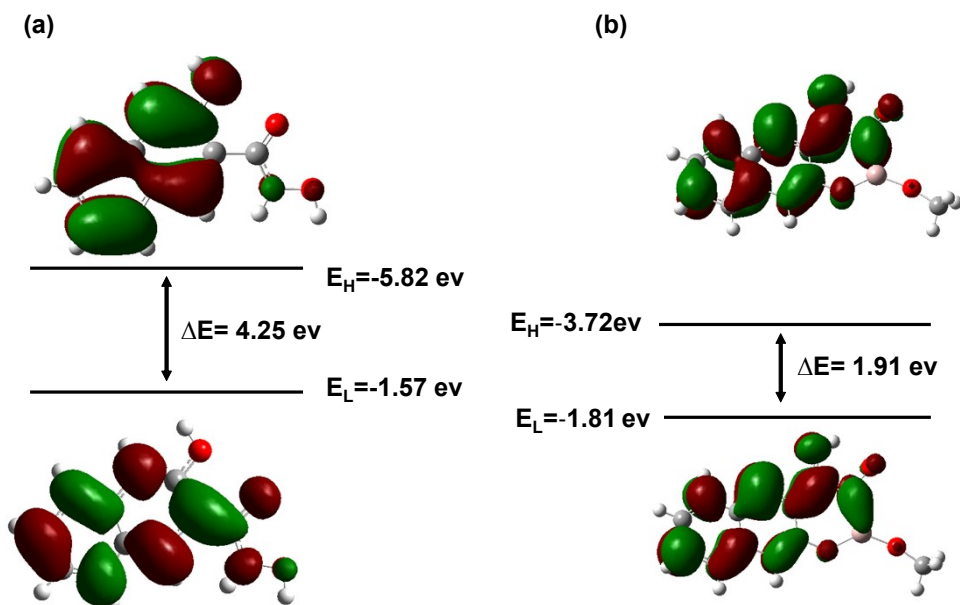


Fig. S14 HOMO and LUMO energies for 1 and 1@Al³⁺.

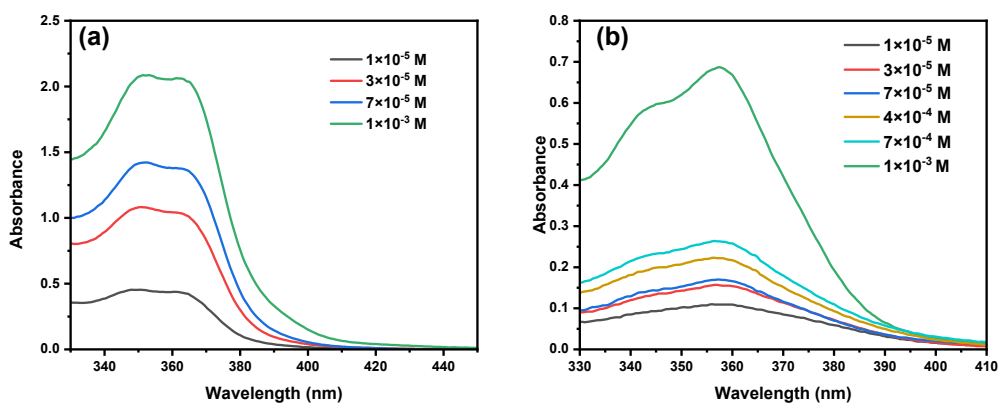


Fig. S15 The absorption spectra of 1 by addition of different concentrations of (a) Al³⁺ and (b) B₄O₇²⁻.

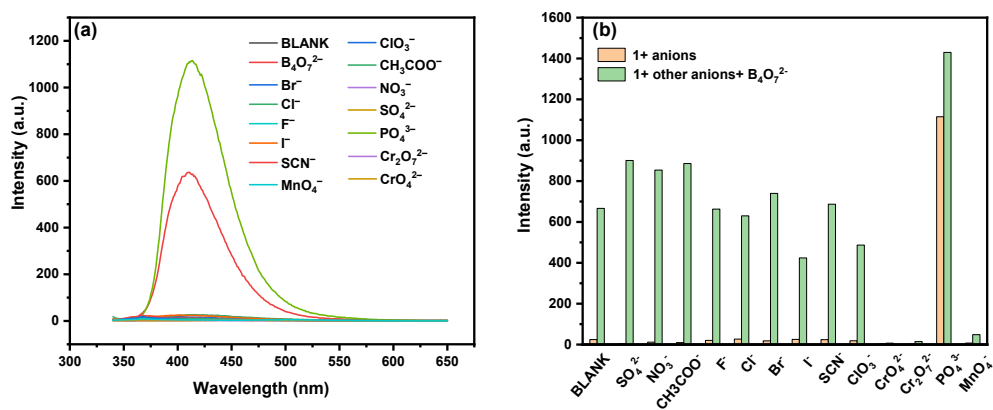


Fig. S16 (a) Luminescence spectra of 1 in solvent (MeOH:H₂O, v/v = 9:1) upon the addition of different non-metal anions; (b) Luminescence intensities at 330 nm of 1 in the presence of only B₄O₇²⁻ (10⁻³ M) and B₄O₇²⁻ with the other non-metal anions (10⁻³ M).

Table S1 The continuous shape measures value calculated using SHAPE 2.1.

Complex	HP(D_{6h})	PPY(C_{5v})	OC(O_h)	TPR(D_{3h})	JPPY (C_{5v})
1	35.956	19.726	5.131	4.439	23.839

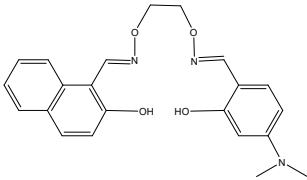
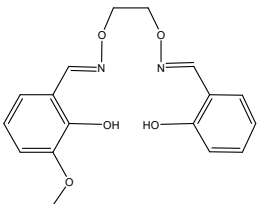
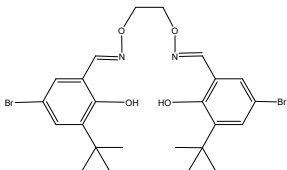
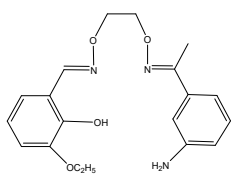
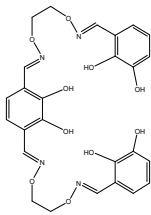
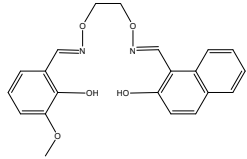
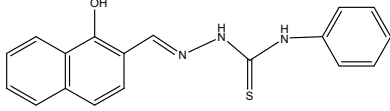
Table S2 Selected bond lengths (Å) for **1**.

Selected bond lengths	
In(1)–O(1)	2.1540(19)
In(1)–O(2)	2.132(2)
N(1)–O(1)	1.372(3)
C(1)–O(2)	1.268(3)
C(1)–N(1)	1.315(3)

Table S3 Comparison of various sensors for the detection of Al^{3+} and $B_4O_7^{2-}$.

	Complex	Sensing type	Identification substance	LOD	Reference
1	A-curcumin@MOF-5	Turn-on	Al^{3+}	3.10 μM	1
2	B-curcumin@MOF-5	Turn-on	Al^{3+}	2.84 μM	1
3	$Eu^{3+}@UiO-66-(COOH)_2/OH$	Turn-off	Al^{3+}	0.36 μM	2
4	$[Zn(ICA)_2(DMF)(H_2O)_3]$	Turn-on	Al^{3+}	0.607 μM	3
5	$\{[Cd(2-amino-1,4-benzenedicarboxylate)(4,4'azopyridine)](DMA)\}_n$	Turn-on	Al^{3+}	0.38 μM	4
6	$\{[Zn_2(NDC)_2(4bppyttz)]1.5DMF\}$	Turn-on	Al^{3+}	2.9 μM	5
7	$In(H_2nha)_3$	Turn-on	Al^{3+}	1.3 μM	This work
8	$\{[Tb(dppa)(H_2O)_2]dima H_2O \cdot 0.5O\}_n$	Turn-on	$B_4O_7^{2-}$	1.49 μM	6
9	$In(H_2nha)_3$	Turn-on	$B_4O_7^{2-}$	6.2 μM	This work

Table S4 Various sensors for the detection of $B_4O_7^{2-}$.

	Fluorescent sensor	Sensing type	The detected anions	Ref
1	$\{[Tb(dppa)(H_2O)_2] \cdot dima \cdot H_2O \cdot 0.5O\}_n$	Turn-on	$B_4O_7^{2-}$, HSO_3^- , CO_3^{2-} , CH_3COO^- , HCO_3^- , $S_2O_3^{2-}$, I^- , S^{2-} , $C_2O_4^{2-}$, Br^- , Cl^- , SO_4^{2-} , NO_2^- , CrO_4^{2-} , $Cr_2O_7^{2-}$	6
2		Turn-on	F^- , Cl^- , Br^- , I^- , HSO_4^- , S^{2-} , SO_3^{2-} , SO_4^{2-} , CO_3^{2-} , HCO_3^- , CN^- , HPO_4^{2-} , $H_2PO_4^-$, $P_2O_7^{2-}$, $B_4O_7^{2-}$, CH_3COO^- , ClO_4^-	7
3		Turn-off	F^- , Cl^- , Br^- , I^- , HPO_4^{2-} , $H_2PO_4^-$, $P_2O_7^{4-}$, S^{2-} , CH_3COO^- , SO_4^{2-} , CO_3^{2-} , HCO_3^- , CN^- , ClO_4^- , $B_4O_7^{2-}$	8
4		Turn-on	$B_4O_7^{2-}$, Cl^- , ClO_4^- , CN^- , CO_3^{2-} , $H_2PO_4^-$, HPO_4^{2-} , HS^- , I^- , NO_2^- , NO_3^- , CH_3COO^- , $P_2O_7^{4-}$, F^- , S^{2-} , Br^- , HCO_3^-	9
5		Turn-off	F^- , Cl^- , Br^- , I^- , ClO_4^- , S^{2-} , HS^- , SO_3^{2-} , $S_2O_8^{2-}$, CO_3^{2-} , SO_4^{2-} , HCO_3^- , CN^- , SCN^- , CH_3COO^- , Ppi , $H_2PO_4^-$, HPO_4^{2-} , NO_2^- , NO_3^- , $B_4O_7^{2-}$	10
6		Turn-on	F^- , Cl^- , Br^- , I^- , ClO_4^- , $H_2PO_4^-$, CN^- , SiO_3^{2-} , CH_3COO^- , $B_4O_7^{2-}$, HS^- , S^{2-} , NO_3^- , CO_3^{2-} , HCO_3^- , HPO_4^- , $P_2O_7^{4-}$, NO_2^-	11
7		Turn-on	F^- , Cl^- , Br^- , I^- , HPO_4^- , $H_2PO_4^-$, $P_2O_7^{4-}$, S^{2-} , CH_3COO^- , CO_3^{2-} , HCO_3^- , CN^- , ClO_4^- , HS^- , NO_2^- , NO_3^- , $B_4O_7^{2-}$	12
8		Turn-on	$B_4O_7^{2-}$, SO_4^{2-} , PO_4^{3-} , NO_3^- , NO_2^- , $P_2O_7^{2-}$, $H_2PO_4^-$, F^- , CH_3COO^- , Br^- , HCO_3^-	13

1. T. Zhong, D. Li, C. Li, Z. Zhang and G. Wang, *Anal. Methods*, 2022, **14**, 2714-2722.
2. Y.-F. Xia, G.-M. Bao, X.-X. Peng, X.-Y. Wu, H.-F. Lu, Y.-F. Zhong, W. Li, J.-X. He, S.-Y. Liu, Q. Fan, S.-H. Li, W. Xiao and H.-Q. Yuan, *Anal. Chim. Acta*, 2022, **1221**, 340115.
3. Z. Zhang, T. Zhong and G. Wang, *J. Photochem. Photobiol., A*, 2022, **431**, 114052.
4. R. Debnath, R. Bhowmick, P. Ghosh, S. Biswas and S. Koner, *New J. Chem.*, 2022, **46**, 8523-8533.
5. X.-C. Huang, Y.-X. Jiang, Z.-J. Han, W. Yong, Q.-X. Huang, W.-X. Shi, X.-R. Chen, J.-J. Kong and H. Wu, *J. Mol. Struct.*, 2023, **1289**, 135897.
6. X.-L. Chen, L. Shang, L. Liu, H. Yang, H.-L. Cui and J.-J. Wang, *Dyes Pigm.*, 2021, **196**, 109809.
7. Y. Huang, Y.-F. Ding, Y.-R. Zheng, Y.-X. Sun and W.-K. Dong, *J. Mol. Struct.*, 2023, **1292**, 136132.
8. X. Xu, Y. J. Li, T. Feng, W. K. Dong and Y. J. Ding, *Luminescence*, 2021, **36**, 169-179.
9. J.-F. Wang, R.-N. Bian, T. Feng, K.-F. Xie, L. Wang and Y.-J. Ding, *Microchem. J.*, 2021, **160**, 105676.
10. W. Guo, T. Ji, Y. Ma, H. Song, J. Liu and W. Dong, *J. Mol. Struct.*, 2023, **1285**, 135545.
11. L.-M. Pu, L. Wang, Z.-L. Wei, Z.-Z. Chen, H.-T. Long, J.-X. Ru and X.-Y. Dong, *Spectrochim. Acta, Part A*, 2021, **249**, 119263.
12. X. Xu, R.-N. Bian, S.-Z. Guo, W.-K. Dong and Y.-J. Ding, *Inorg. Chim. Acta*, 2020, **513**, 119945.
13. Y. Chen, L. Jin, W. Wang, L. Dai, X. Tan and Q. Wang, *ChemistrySelect*, 2019, **4**, 2379-2382.